DOI: 10.1002/hlca.201800229

FULL PAPER

HELVETICA chimica acta

Label-Free Quantification of 5-Azacytidines Directly in the Genome

Sarah Schiffers,[a] Thomas M. Wildenhof,[a] Katharina Iwan,[a] Michael Stadlmeier,[a] Markus Müller,[a] and Thomas Carell*[a]

[a] Center for Integrated Protein Science at the Department of Chemistry, Ludwig-Maximilians-Universität München, Butenandtstr. 5–13, DE-81377 München, e-mail: Thomas.Carell@lmu.de

Dedicated to Prof. *François Diederich*

Azacytidines (AzaC and AzadC) are clinically relevant pharmaceuticals that operate at the epigenetic level. They are integrated into the genome as antimetabolites to block DNA methylation events. This leads to a reduction of the 5-methyl-2′-deoxycytidine (m^5dC) level in the genome, which can activate epigenetically silenced genes. Because of the inherent chemical instability of Aza(d)Cs, their incorporation levels in DNA and RNA are difficult to determine, which hinders correlation of therapeutic effects with incorporation and removal processes. Existing methods involve radioactive labeling and are therefore unsuitable to monitor levels from patients. We report here a new direct chemical method that allows absolute quantification of the levels of incorporated AzaC and AzadC in both RNA and DNA. Furthermore, it clarifies that Aza(d)C accumulates to high levels (up to 12.9 million bases per genome). Although RNA-based antimetabolites are often 2′-deoxygenated *in vivo* and incorporated into DNA, for AzaC we see only limited incorporation into DNA. It accumulates predominantly in RNA where it, however, only leads to insignificant demethylation.

Keywords: mass spectrometry, leukemia, DNA methylation, azacytidine, DNA methyltransferases.

Introduction

Methylation of deoxycytidines in genomic CpG context creates methylated palindromic (^{m}CpG) sites, which trigger the silencing of gene expression.[1] Silencing of tumor suppressor genes in turn is a hallmark of cancer.[2] Others and us could recently show, that the inability to remove methyl marks from ^{m}CpG-islands is a problem in many tumors that helps maintaining uncontrolled cell division and hence tumor growth.[3] The RNA nucleoside 5-Azacytidine (AzaC) and its corresponding DNA analogue 5-Aza-2′-deoxycytidine (Decitabine, AzadC) are pharmaceuticals, which are in clinical use for the treatment of myelodysplastic syndromes (MDS) and acute myeloid leukemia (AML).[4–6] These compounds are prodrugs, which are converted into the corresponding triphosphates and incorporated into both DNA and RNA at levels that are difficult to measure and therefore often unknown.[7,8] Once incorporated, they function as suicide inhibitors of methyltransferases (Dnmt1 and 3a/3b) as depicted in *Scheme 1,a*.[9–12] This inhibitory effect leads to a global reduction of the m^5dC levels in DNA[13] and consequently to a reactivation of silenced tumor-suppressor genes.[14,15] Methylation of cytidine bases (m^5C) occurs also in RNA, and is performed by Dnmt2[16] and specific NOP2/Sun domain family proteins (NSUN2[17], 4,[18] and 6[19]). The question to which extent inhibition of methylation in RNA contributes to the clinical effect of AzaC treatment is unanswered. A recent meta-analysis seems to back up previous findings,[20–22] that AzaC gives slightly better clinical results than AzadC.[23] The molecular cause however remains elusive, especially considering the fact that AzaC first has to be reduced by ribonucleotide reductase to enter DNA. Accordingly, it is important to investigate the levels at which AzadC and AzaC are integrated into nucleic acids.

Supporting information for this article is available on the WWW under https://doi.org/10.1002/hlca.201800229

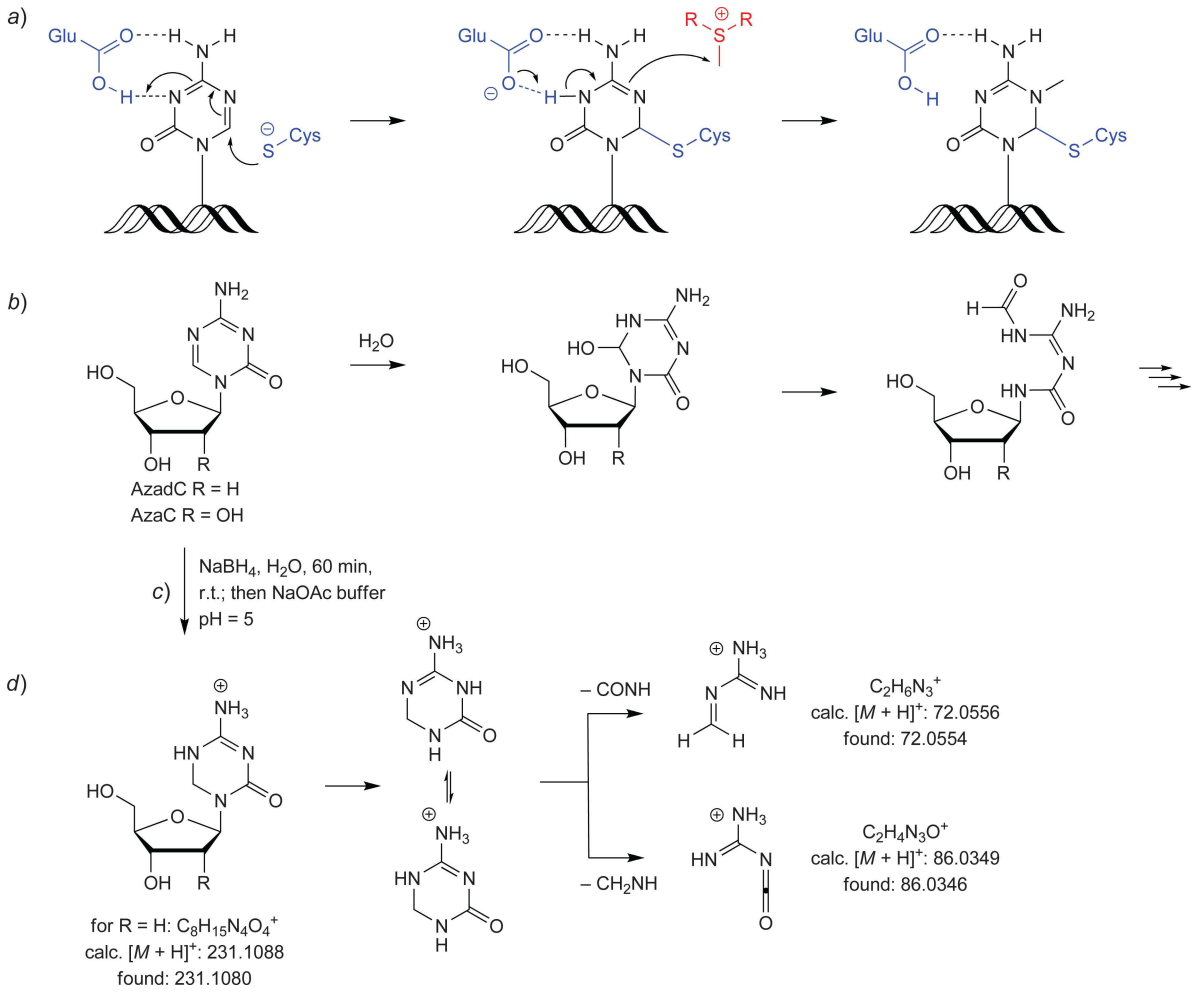

Scheme 1. *a*) Proposed mechanism of action of 5-Azacytidine (Aza(d)C). The blue components are part of the active site of the DNA methyltransferases (DNMTs). The active part of the SAM cofactor is depicted in red. *b*) Depiction of the main hydrolysis pathway of Aza(d)C. *c*) Stabilization of AzadC by $NaBH_4$ reduction and *d*) fragmentation pathway of H_2–AzadC with the calculated and found *m/z* values in MS^2 experiments.

A major problem associated with the analysis of the incorporation efficiencies is the hydrolytic instability of the Aza(d)C compounds, which feature reported half-life times between 3.5 h and 21 h.[24,25] This makes the direct measurement of the compounds in DNA and RNA impossible. Feeding of radioactive Aza(d)C is only of limited use due to its instability because one is unable to distinguish intact integrated material from chemically unreactive fragments that are still present in DNA and RNA.[26] In light of observed resistance phenomena in treated patients, there is a great need for a direct analytic method that can give levels of intact AzadC and AzaC in DNA and RNA.[27,28]

Results and Discussion

The instability of Aza(dC) is caused by its electrophilic character, which allows water to attack the C(6) position as depicted in *Scheme 1,b*. This is followed by opening of the hemiaminal substructure and subsequent deformylation and deribosylation.[24][25] We rationalized that any analysis of intact Aza(d)C after DNA or RNA isolation would require immediate stabilization of the incorporated compounds to stop further degradation during DNA and RNA isolation and handling.

We found that treatment of Aza(d)C with $NaBH_4$[29–32], is a very efficient reaction that leads to the formation of the corresponding dihydro–Aza(d)C (H_2–Aza(d)C) compounds. We furthermore discovered that despite the lack of any aromaticity, these

compounds are surprisingly stable. When we reacted the Aza(d)C nucleoside with aqueous $NaBH_4$ followed by elimination of borate with acetate buffer (pH = 5, *Scheme 1,c*) we noted full conversion to the corresponding stabilized H_2–Aza(d)C versions already after 60 min reaction at room temperature (*Figure SI-6 A* in the *Supporting Information*). A long-term NMR study showed that H_2–AzadC is stable in D_2O at 37 °C for several hours (*Figure SI-4*), while the original AzadC shows 16% decomposition already after 6 h. In order to enable LC–MS based quantification, we next analyzed the MS fragmentation patterns of H_2–AzadC (*Scheme 1,d*). The positively charged precursor ion with a mass-to-charge ratio (*m/z*) of 231 fragments first through cleavage of the glycosidic bond. The base heterocycle seems to exist in two tautomeric forms in the gas phase, which undergo retro-*Diels-Alder* fragmentations under elimination of either –HNCO or $-CH_2NH$. This leads to clearly detectable fragment ions with *m/z* of 72 and *m/z* 86 (*Figure SI-7*). This mechanistic assumption is supported by a study with a monodeutero-H_2–AzadC derivative (*Figure SI–8*, *Scheme SI–1*). We then developed a UHPLC method to separate H_2–Aza(d)C from the canonical nucleosides and modified the enzymatic digestion protocol[33] enabling digestion of DNA and RNA and liberating H_2–Aza(d)C completely (*Figure SI-10–SI-12*). This method was further validated with different amounts of DNA. A similar method that uses a different sample preparation and a different mass spectrometric method was recently published.[31]

Next, we evaluated the new method in realistic scenarios using AzadC-treated cells. For the study, we used leukemia model cell lines and AzadC concentrations of up to 1 μM. The first study was performed with the leukemia model cell line HL60, which are promyeloblast cells derived from acute promyelocytic leukemia. A second study was performed with the AML cell line MOLM-13 (*Figure 1*). In both cases, the cells were cultured in the presence of increasing concentrations of AzadC for 24 h, which is longer than the half-life of the compound in solution.[24,25] The DNA was isolated, treated with $NaBH_4$, subsequently fully digested and analyzed by UHPLC-MS^2 using the developed protocol.

To our delight, we detected a clear and strong signal for the H_2–AzadC using our method. The signal intensity nicely increased in a dose-dependent manner (*Figure 1*, green bars), proving the presence of intact AzadC in the genome. Using external calibration curves of the H_2–AzadC standard subjected to our optimized digestion conditions, it was now possible to perform exact quantification (*Figure SI-10*). We found about 2000 AzadC per million nucleotides when we supplemented with AzadC (1 μM). This corresponds to a rather high level of 12.9 million AzadCs per genome. These high levels may be due to a higher stability of the genome-incorporated AzadC compared to the corresponding free nucleoside, possibly due to shielding of the compound inside the genomic DNA duplex from reaction with water. Indeed, the AzadC content in isolated DNA was more stable (half-life time of 68.7 h at r.t. (*Figure SI-15*)) than the reported half-life time of the nucleoside.[25] However, we strongly recommend performing the $NaBH_4$ treatment as early as possible. We quantified m^5dC in parallel (*Figure 1*, yellow bars), and confirmed that the increase of AzadC goes in hand with a decline of m^5dC as expected, due to the suicide inhibition of the DNA methyl transferases.

We next investigated the effect of AzadC on cells that undergo significant epigenetic reprogramming to see if we could obtain time-dependent data. For these studies, we treated J1 mouse embryonic stem cells

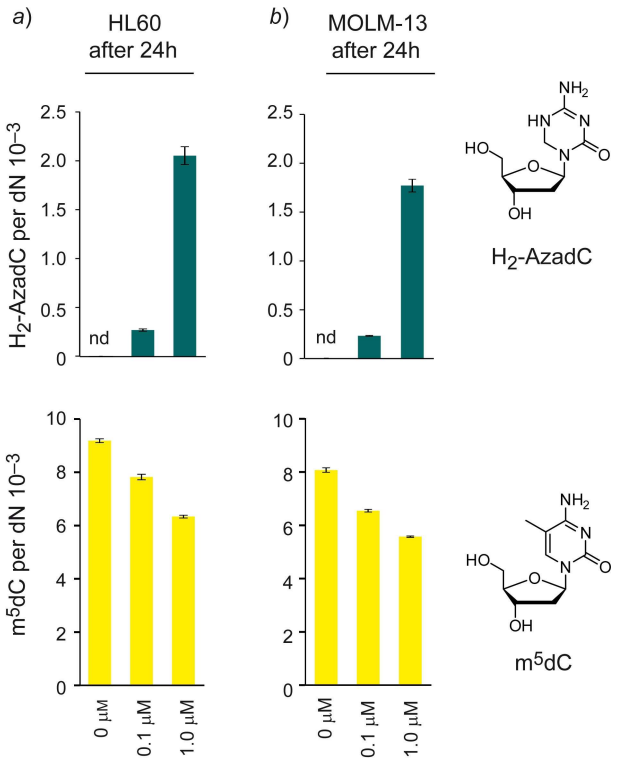

Figure 1. Levels of H_2–AzadC after a 24 h treatment with different concentrations of AzadC. H_2–AzadC (green), m^5dC (yellow) per dN in *a*) HL60 cells, *b*) MOLM-13 cells. nd: not detected. Error bars indicate standard deviation of three independent biological replicates.

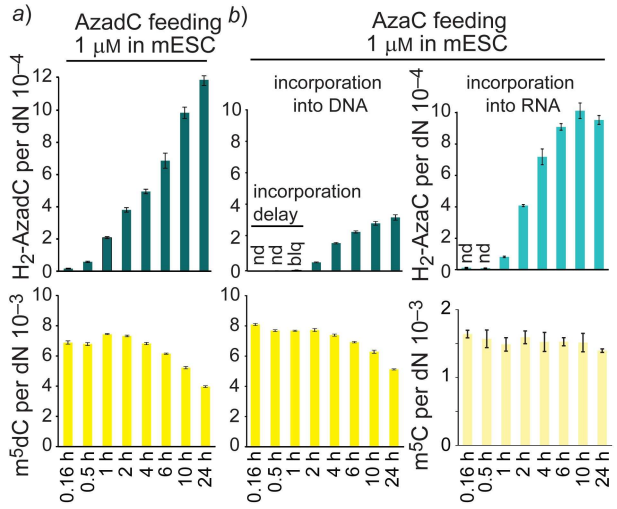

Figure 2. Levels of H_2–AzadC (*a*) and H_2–AzaC (*b*) in mESC after drug treatment (1 μM Aza(d)C) over a period of 24 h. After the indicated time points the cells were harvested and the DNA was isolated and analyzed as described. H_2–AzadC (dark green), m^5dC (yellow), H_2–AzaC (light green) and m^5C (light yellow). nd: not detected; blq: below limit of quantification. Error bars indicate standard deviation obtained from three independent biological replicates.

(mESC) with AzadC (1 μM) during the shift from the naïve to the primed state.[34–36] We analyzed the incorporation at different time points (*Figure 2,a*). Indeed, isolation and analysis of the DNA shows an immediate sharp increase of AzadC in the genome that did not reach saturation even after 24 h. Interestingly we noted that despite the immediate integration of AzadC into the genome, a decline of the m^5dC values is first observed after 4 h. This observation is difficult to rationalize but it may explain why also in the clinic, long treatment times are essential for therapeutic success. The biochemical reason for this lag phase needs further investigation.

Furthermore, we started to study if our new method would also allow us to determine the incorporation of the ribo-version AzaC into DNA and RNA. We therefore investigated the effect of the AzaC (1 μM) in the mESC model. We first detected again the deoxygenated version AzadC in the genome, showing that 2′-deoxygenation of AzaC occurs and leads to incorporation of AzadC (*Figure 2,b*). However, the detected levels of H_2–AzadC are reduced by a factor of about four (330 instead of 1200 H_2–AzadC per million nucleotides) and the incorporation is time delayed. The lag phase of 2 h may be attributed to the time needed by the cells to deoxygenate AzaC.[7] The low incorporation yield is most likely to be caused by decreased availability of the 2′-deoxygenated nucleoside due to the incorporation into RNA and therefore reduction of the soluble pool. Our finding also matches a recent publication[37], in which the ribonucleotide reductase was identified as an AzaC target leading to reduction of the 2′-deoxy-nucleoside pool and therefore probably arrest of the replication.

To our surprise, despite the lower incorporation level, the onset of m^5dC reduction is again observed after 4 h and the total decline of m^5dC is similar compared to feeding of AzadC. This observation is very interesting and it raises the question of why the observed demethylation is not dose-dependent. From the same sample, we also investigated the levels of the non-deoxygenated AzaC in RNA using a slightly modified UHPLC-MS^2 method. Here we exploit again that the reduction with $NaBH_4$ gives a stable derivative (*Figure SI-5*, *SI-6B*) with a unique high resolution MS fragmentation pattern (*Figure SI-9*).

The detected levels of H_2–AzaC in RNA correspond to 1000 AzaC per million nucleotides after 24 h, which is comparable to the H_2–AzadC levels in DNA after AzadC treatment. The total amount of incorporated nucleotides is consequently very similar, independent of the supplemented Aza(d)C compound, arguing that maybe proper triphosphate generation could be rate determining *in vivo*. In RNA, m^5C does not appear to be significantly reduced upon AzaC feeding, clarifying that demethylation of RNA is likely not responsible for any therapeutic effects.

We conclude that ribosomal m^5C represents the vast bulk of the detected material since knockout of Dnmt2, which is known to methylate tRNA, shows only a slight and insignificant effect on global m^5C levels (*Figure 3,a*). It seems that in RNA, efficient inhibition of the NSUN-methyltransferases does not occur.

In DNA however, Aza(d)C mediated demethylation appears largely unaffected by the available methyltransferase. We find that equally strong demethylation occurs in all investigated DNMT knockouts, despite efficient incorporation of AzadC into their genomes (*Figure 3,b*). This is somewhat surprising, since inhibition of the maintenance methyltransferase DNMT1 is considered to have the strongest impact on global m^5dC levels.[38]

Conclusions

Here, we report two new mass spectrometry-based methods for the exact quantification of AzadC and AzaC in DNA and RNA. Importantly, the methods allow

quantification of m^5dC in parallel with H_2–AzadC and m^5C in parallel with H_2–AzaC, respectively. This now enables us to correlate incorporation efficiencies with the expected biochemical effect, namely reduction of the $m^5(d)C$ values. Using the new method, we learned that AzaC is efficiently 2′-deoxygenated to AzadC. Both compounds lead to comparable reductions of the m^5dC levels, but not in a dose-dependent manner and only after a significant lag time. Interestingly, we did not see a significant reduction of the m^5C values upon feeding of AzaC, despite its efficient incorporation into RNA, arguing that depletion of RNA methyltransferase may not be accomplished as easily as of DNA methyltransferases. It may also hint at an alternative mechanism of Aza(d)C-mediated demethylation, which acts through replacement of m^5dC by DNA repair processes, rather than inhibition of maintenance methylation. The absence of equivalent repair mechanisms in RNA adds further support to this hypothesis. Given the generally lower DNA incorporation rate in case of AzaC, its particular beneficial effects[23] may arise from the incorporation into RNA rather than DNA. Most importantly, the new methods do not rely on radioactive labeling and can consequently be used to monitor the effects directly in samples from patients treated with Aza(d)C and moreover allow distinguishing catabolic by-products from the intact drug. This now paves the way to study the pressing resistance problems associated with epigenetic Aza(d)C therapy.

Experimental Section

Chemical Synthesis – General Methods

Preparative HPLC: *Waters 1525* Binary HPLC Pump, *2487* Dual λ Absorbance Detector; *Macherey-Nagel VP 250/10 Nucleosil 100-7-C18*; flow rate 5 mL/min.

Analytical HPLC: *Waters 2695* Separation Module, *2996* Photodiode Array Detector; *Macherey-Nagel* EC *250/4 Nucleosil 120-3-C18*; flow rate 0.5 mL/min.

^1H- and ^{13}C-NMR spectra were recorded with a *Bruker Avance III HD 400* MHz spectrometer equipped with a CryoProbe. Chemical shifts are expressed in parts per million [ppm] and indicated relative to tetramethylsilane (TMS). The deuterated solvents D_2O served thereby as internal standards. Spin multiplicities are indicated as follows: *s* (*singlet*), *d* (*doublet*), *t* (*triplet*), *q* (*quartet*), *m* (*multiplet*) and combinations thereof. Signals were assigned to their respective source through informally allocated atom numbers. Structural analysis was conducted with ^1H- and ^{13}C-NMR spectra under the aid of additional 2D spectra (COSY, HMBC, and HSQC). Spectral analysis was conducted with the software MestReNova v.9.1.0–14011 from *Mestrelab Research S.L.*

The high-resolution mass spectrometer for chemicals was operated by the section for mass spectrometry of the department chemistry and pharmacy, LMU Munich. The spectra were acquired through electro spray ionization (ESI) with a *Finnigan LTQ FT* from *Thermo Finnigan GmbH*. Either the molecule ion signal or the signal of another characteristic fragment is indicated in the analysis section of each product.

Melting temperatures were acquired with a *BÜCHI* Melting point *B-450* from *BÜCHI Labortechnik AG* and are uncorrected.

Synthesis of 5,6-Dihydro-5-aza-2′-deoxycytidine (= **4-Amino-1-[(2*R*,4*S*,5*R*)-4-hydroxy-5-(hydroxymethyl)-oxolan-2-yl]-5,6-dihydro-1,3,5-triazin-2(1*H*)-one**; H_2–AzadC). The procedure was modified from a previous publication.[30] In detail, a freshly prepared solution of $NaBH_4$ (9.95 mg, 262.9 μmol, 4 equiv.) in H_2O (1.5 mL) was added to AzadC (15.0 mg, 65.7 μmol,

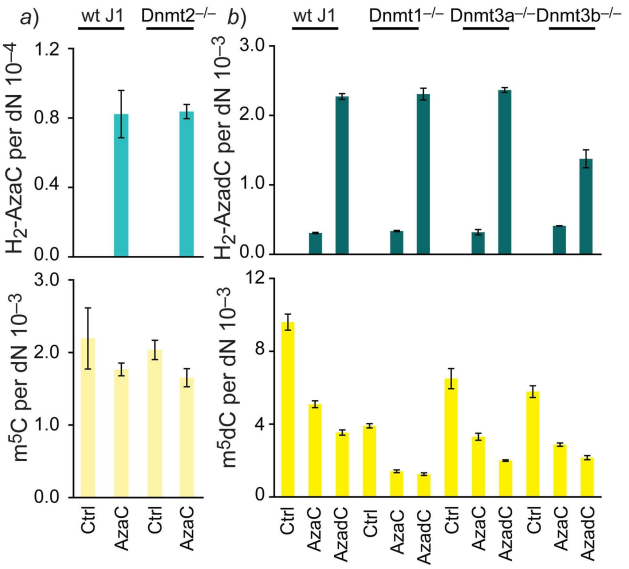

Figure 3. Incorporation of AzadC and AzaC into RNA *a*) and DNA *b*) of various DNMT knock-out mESCs 24 h after drug treatment (1 μM). H_2–AzadC (dark green), m^5dC (yellow), H_2–AzaC (light green), and m^5C (light yellow). nd: not detected. Error bars indicate standard deviation obtained from three independent biological replicates.

1.0 equiv., *Carbosynth Limited*) and stirred 1.5 h at r.t. The reaction was quenched with aqueous NaOAc-Buffer (0.5 mL, 750 mM, pH = 5), and the resulting mixture was stirred for 1 h. The mixture was filtered with a syringe filter (*Acrodisc*® 13 mm, 0.2 μm, *GHP Membrane*, *PALL Laboratory*) and directly subjected to preparative HPLC purification and collected as broad peak at $t = 4.8$ min (100% H_2O in 25 min). The obtained fractions were pooled and the solvent was removed by lyophilization on a *Christ Alpha L–D* plus to afford H_2–AzadC as colorless powder. (14.9 mg, 64.7 μmol, 98%). M.p.: over 230 °C, decomposition. ^{1}H-NMR (400 MHz, D_2O): 6.22 (*dd*, *J* = 8.2, 6.5, 1 H); 4.66–4.53 (*m*, 2H), 4.38–4.31 (*m*, 1 H); 3.94–3.82 (*m*, 1 H); 3.75 (*dd*, *J* = 12.3, 4.0, 1 H); 3.67 (*dd*, *J* = 12.3, 5.3, 1 H); 2.25 (*ddd*, *J* = 14.6, 8.2, 6.6, 1 H); 2.06 (*ddd*, *J* = 14.2, 6.5, 3.4, 1 H). ^{13}C-NMR (101 MHz, D_2O): 160.3; 159.3; 84.9; 83.7; 70.9; 61.6; 50.9; 35.1. HR-ESI-MS: 231.1088 ($[C_8H_{15}N_4O_4]^+$, $[M+H]^+$; calc. 231.1088).

Synthesis of 6-Deutero-5-hydro-5-aza-2′-deoxycytidine (= **4-Amino-1-[(2*R*,4*S*,5*R*)-4-hydroxy-5-(hydroxymethyl)oxolan-2-yl](6-^{2}H$_1$)-5,6-dihydro-1,3,5-triazin-2(1*H*)-one**; MH_2–AzadC). The synthesis was performed analogous to H_2–AzadC with $NaBD_4$ (11.0 mg, 262.9 μmol, 4.0 equiv.) as reducing agent and afforded 6-monodeutero-5-hydro-5-aza-2′-deoxycytidine (MH_2–AzadC; 14.6 mg, 63.1 μmol, 96%) as colorless powder. M.p.: over 230 °C, decomposition. ^{1}H-NMR (400 MHz, D_2O): 6.17 (*dd*, *J* = 8.1, 6.6, 1 H); 4.52 (*d*, *J* = 9.2, 1 H); 4.34–4.25 (*m*, 1 H); 3.88–3.79 (*m*, 1 H); 3.69 (*dd*, *J* = 12.3, 3.9, 1 H); 3.61 (*dd*, *J* = 12.2, 5.3, 1 H); 2.19 (*ddd*, *J* = 14.6, 8.2, 6.7, 1 H); 2.04 (*ddd*, *J* = 14.1, 6.4, 3.4, 1 H). ^{13}C-NMR (101 MHz, D_2O): 160.5; 159.4; 84.8; 83.6; 70.9; 61.5; 50.5 (*t*, 1 C); 34.97. HR-ESI-MS: 232.1151 ($[C_8H_{14}DN_4O_4]^+$, $[M+H]^+$; calc. 232.1151).

Synthesis of 5,6-dihydro-5-azacytidine (= **4-Amino-1-[(2*R*,3*R*,4*S*,5*R*)-3,4-dihydroxy-5-(hydroxymethyl)oxolan-2-yl]-5,6-dihydro-1,3,5-triazin-2(1*H*)-one**; H_2–AzaC). The procedure was modified from a previous publication.[30] In detail, a freshly prepared solution of $NaBH_4$ (9.29 mg, 245.6 μmol, 4 equiv.) in H_2O (1.5 mL) was added to AzaC (15.0 mg, 61.4 μmol, 1.0 equiv., *Sigma-Aldrich*) and stirred 1.5 h at r.t. The reaction was quenched with aqueous HCl (0.5 mL, 0.5 M), and the resulting mixture was stirred for 30 min. The mixture was brought to pH = 10 with aqueous NH_4OH (5%) and stirred for another 30 min. After filtration with a syringe filter (*Acrodisc*® 13 mm, 0.2 μm, *GHP Membrane*, *PALL Laboratory*), the mixture was directly subjected to preparative HPLC purification and collected as broad peak at $t = 5.2$ min. (100% H_2O in 25 min) The obtained fractions were pooled and the solvent was removed by lyophilization on a *Christ Alpha L–D* plus to afford 5,6-dihydro-5-azacytidine (H_2–AzaC) as colorless powder (14.7 mg, 59.7 μmol, 97%). M.p.: over 219 °C, decomposition. ^{1}H-NMR (400 MHz, D_2O): 5.64 (*d*, *J* = 6.8, 1 H); 4.52–4.44 (*m*, 2H), 4.14–4.08 (*m*, 1 H); 4.00 (*dd*, *J* = 5.7, 3.6, 1 H); 3.88–3.82 (*m*, 1 H); 3.64 (*dd*, *J* = 12.5, 3.5, 1 H); 3.56 (*dd*, *J* = 12.5, 4.7, 1 H). ^{13}C-NMR (101 MHz, D_2O): 160.0; 159.0; 87.1; 83.1; 70.06; 70.04; 61.3; 51.3. HR-ESI-MS: 247.1037 ($[C_8H_{15}DN_4O_5]^+$, $[M+H]^+$; calc. 247.1037).

Long-Term NMR Study of the Stability of the Compound

A sample of the synthetic H_2–AzadC or AzadC, or H_2–AzaC and AzaC respectively (*ca.* 1 mg) was dissolved in D_2O (1 mL, *Eurisotop*) and immediately subjected to ^{1}H-NMR. The NMR-tube with the sample was then incubated in a water bath at 37 °C and measured after indicated times. After that, the sample was left at r.t. and measured again. For AzadC, integrals of peaks from H–C(1′) are indicated, after 6 h at 37 °C, a decay of approximately 16% of the compound can be observed (*Figure SI-4*). For AzaC, integrals of peaks from H–C(1′) are indicated, after 18 h at 37 °C, a decay of approximately 37% of the compound can be observed (*Figure SI-5*).

HPLC Conversion Studies

A freshly prepared solution of $NaBH_4$ in H_2O (0.5 mL, 250 mM) was added to AzadC (*A*) or AzaC (*B*) (1.00 mg, 4.4 μmol, 1.0 equiv., *Carbosynth Limited*) and stirred at r.t. After 60 min, the mixture (100 μL) was quenched with NaOAc-Buffer (50 μL, 750 mM, pH = 5) and placed in an *Eppendorf Thermomix* comfort at 22 °C and 600 rpm shaking to remove hydrogen bubbles from the reaction. After short-spin centrifugation, the mixture was diluted 1:10 and subjected to analytical HPLC. 0→5% MeCN in H_2O, 0→25 min; 5%→80%, 25 min→28 min; 80%→80%, 28 min→38 min; 80%→0%, 38 min→45 min. As control, AzadC or AzaC was diluted in H_2O and immediately subjected to analytical HPLC with the same mobile phase gradient (*Figure SI-6*).

HR-MS-Fragmentation

Fragmentation experiments were conducted on an *Orbitrap XL* mass spectrometer (*Thermo Fisher Scientific*), equipped with a *HESI-II-ESI* source (*Thermo Fisher*

Scientific). A solution of the sample in water was directly injected using a syringe pump with a flow rate of 3 μL/min (H_2–AzaC) or 5 μL/min (H_2–AzadC, MH_2–AzadC). Spray parameters are given in *Table SI-5*. The isolation window was set to 1 *m/z*. High-resolution mass spectra were recorded manually with a resolution of 30000 in a mass range from 60 *m/z* to 250 *m/z*. MS^2 and MS^3 spectra for H_2–AzadC and MH_2–AzadC were recorded with a normalized collision-induced dissociation energy of 20% with a resolution of 30000 in a mass range from 50 *m/z* to 250 *m/z*. In the case of H_2–AzaC, MS^2 spectra were acquired with a normalized higher-energy collisional dissociation energy of 30% with a resolution setting of 30000 in a mass range from 65 *m/z* to 300 *m/z*.

To gain a more accurate mass, after acquisition several spectra were summarized in the Xcalibur QualBrowser (*Thermo Fisher Scientific*; *Figure SI-7*). The proposed fragmentation pathway of MH_2–AzadC is depicted in *Scheme SI-1*, and complementary to the unlabeled H_2–AzaC (*Scheme SI-2*).

Cell Culture and Drug Treatment

5-Azacytidine (*Sigma-Aldrich*) and 5-Aza-2′-deoxycytidine (*Carbosynth*) were dissolved as dimethyl sulfoxide (DMSO) stocks (100 mM) and stored frozen at −80 °C. For treatment of mESC, this stock was diluted to a concentration, that when applied to cell culture medium, the final DMSO concentration did not exceed 1%. Due to the sensitivity of the HL60 cells to DMSO, the DMSO stocks (100 mM) were diluted with ddH_2O (to 100× the final concentration) and then directly applied to the culture medium.

Cancer Cell Lines

HL60 cells (*ATCC*) and MOLM-13 (*Leibniz Institute DSMZ-German Collection of Microorganisms and Cell Cultures*) were cultured in *RPMI-1640* Medium (*Sigma-Aldrich*) supplemented with 20% fetal bovine serum (FBS, *Life Technologies*), L-alanyl-L-glutamine (2 mM, *Sigma-Aldrich*) and a mixture of penicillin and streptomycin (100 U/mL, 100 μg/mL, 1×, *Life Technologies*). HL60 cells are promyeloblast cells derived from an acute promyelocytic leukemia, MOLM-13 is an acute myeloid leukemia cell line.[39–41] Cells were incubated in a humidified 37 °C incubator supplied with 5% CO_2. For drug treatment, 4×10^6 cells were suspended in culture medium (4 mL) with Aza(d)C and incubated for 24 h in a P60 cell culture dish (*Sarstedt*). The medium was removed by centrifugation (3 min, 260 *g*) and the cells were washed with phosphate buffered saline (PBS, *Sigma-Aldrich*) and centrifuged again. The pellet was lysed with guanidinium isothiocyanate buffer (1.6 mL, RLT Buffer, *Qiagen*) supplemented with β-mercaptoethanol (final concentration 142 μM, *Sigma-Aldrich*) and subjected to DNA isolation. All cell culture experiments were done in independent biological triplicates.

Mouse Embryonic Stem Cells (mESC)

J1 wt mESCs[42] were maintained in DMEM high glucose (4500 mg/L glucose, sodium pyruvate, and sodium bicarbonate, without L-glutamine, *Sigma-Aldrich*) supplemented with 10% ESC tested FBS (*PAN Biotech*), 1× MEM nonessential amino acids (*Sigma-Aldrich*), L-alanyl-L-glutamine (2 mM, *Sigma-Aldrich*), β-mercaptoethanol (0.1 mM), leukemia inhibitory factor (LIF 1000 U/mL, *ORF Genetics*), and 100 U/mL penicillin with 100 μg/mL streptomycin (*Life Technologies*). For maintaining mESC in the undifferentiated, naive pluripotent state, so called 2i conditions, MEK and GSK3 pathway inhibitors were applied. Therefore, the mESC medium was supplemented with *PD 0325901* (1 μM) and *CHIR 99021* (3 μM, *Axon Medchem*). For all experiments, mESCs were trypsinized with trypsin (0.1%, *Gibco, LifeTechnologies*) in phosphate buffered saline (*Sigma-Aldrich*) containing EDTA (0.02%, *Sigma-Aldrich*), D-glucose (0.01%, *Sigma-Aldrich*) and chicken serum (1%, *Gibco, LifeTechnologies*) and plated in culture dishes pretreated with gelatin (0.2%). mESCs were incubated in a humidified 37 °C incubator supplied with 5% CO_2. For drug treatment, cells were moved into the primed state by removing 2i from the medium. Cells were incubated 2 d in medium without 2i in *P60* cell culture dishes (*Sarstedt*). After splitting, 4×10^5 cells were transferred into a 6-well plate culture dish (*VWR*) and incubated additional 2 d without 2i. Then the medium was replaced with Aza(d)C supplemented medium and incubated for another 24 h. The medium was removed and cells were washed with PBS. Then they were directly lysed with RLT Buffer (*Qiagen*) supplemented with β-mercaptoethanol (final concentration 142 μM, *Sigma-Aldrich*) and subjected to DNA isolation.

For comparison of J1 wt mESCs with the respective Dnmt1,[43] Dnmt2,[44] Dnmt3a,[44] and Dnmt3b[44] knockout cell lines the culturing procedure was the same as described above, but after the first passage in

serum/LIF conditions without 2i only 2×10^5 cells were plated per 6-well.

DNA and RNA Isolation

DNA was isolated from cell lysates using *Zymo-Spin™ V* spin columns (*ZymoResearch*), according to the manufacturers' manual with following variation. After DNA binding columns were incubated 5 min with Genomic Lysis Buffer (*ZymoResearch*) supplemented with RNAse A (35 U/mL, *Qiagen*). After the washing steps, DNA was eluted from the column with ddH_2O (100–150 μL) containing 3,5-di-*tert*-butyl-4-hydroxy-toluene (BHT, 0.2 μM) and the concentration was determined on a *NanoDrop ND-1000* Spectrophotometer (*NanoDrop Technologies Inc.*).

RNA was isolated from the flow-through of DNA isolations using *ZR-Duet™* DNA/RNA *MiniPrep Kit* (*ZymoResearch*) according to the manufacturer's manual.

$NaBH_4$ Reduction of Isolated DNA and RNA

The DNA or RNA (10 μg) was diluted with ddH_2O (up to 75 μL). A freshly prepared solution of $NaBH_4$ (25 μL, 1 M) was added to the sample (final concentration of 250 mM $NaBH_4$) and incubated in the dark in a *Eppendorf Thermomix* comfort at 22 °C and 600 rpm interval shaking (20 s shake, 9 min 40 s interval) for 4 h. This treatment was previously reported[30] in different conditions and was modified to work in water. Its compatibility with genomic DNA was previously shown.[45] Then NaOAc buffer (50 μL, 750 mM, pH = 5) was added carefully to each sample to quench the excess of borohydride and incubated at 22 °C for 2 h at 600 rpm. Remaining hydrogen bubbles were removed by short-spin centrifugation and the DNA was purified and re-isolated using *Zymo-Spin™ IIC–XL* spin columns (*ZymoResearch*) according to the manufacturer's manual. The DNA was eluted in ddH_2O (60 μL) and the DNA concentration was determined. RNA was re-isolated accordingly using the *Zymo-Spin™ IIC spin* columns (*ZymoResearch*) according to the manufacturer's manual.

Enzymatic DNA and RNA Digest

DNA and RNA samples were digested to give a nucleoside mixture and spiked with specific amounts of the corresponding isotopically labeled standards before LC–MS/MS analysis. The enzymatic digest method was slightly modified from our previous reported method.[33] Especially TRIS-buffer salts contributed heavily to ion suppression of H_2–AzadC and H_2–AzaC MS-signals. DNA or RNA (1 μg) was incubated for 3 h at 37 °C in technical triplicate with S1 nuclease (*Sigma-Aldrich*) and Antarctic Phosphatase (*New England BioLabs*) as stated in our reported methods. For RNA, the amount of $ZnSO_4$ was increased (1.6 mM in 7.5 μL), and $MgCl_2$ (2.67 mM in 7.5 μL) was added additionally. Subsequently, for DNA Snake Venom Phosphodiesterase I (*Abnova*) in a glycerol stock was added according to the manufacturer omitting the addition of TRIS-buffer salts and the solution was incubated for another 3 h at 37 °C. For RNA, the first S1/Antarctic Phosphatase addition and incubation was repeated for another 12 h at 37 °C.

UHPLC-MS/MS Analysis

Experimental procedures for synthesis, purification, stock solution preparation, and determination of extinction coefficients for the isotopic nucleoside standards were reported earlier by our group.[33,46–48] In brief, LC-ESI-MS/MS analysis was performed using an *Agilent 1290 UHPLC* system, equipped with an UV-detector, and an *Agilent 6490* triple quadrupole mass spectrometer coupled with the stable isotope dilution technique. The nucleosides were analyzed in the positive ion selected reaction monitoring mode (SRM). In the positive ion mode $[M+H]^+$ species were measured. The optimized general source-dependent parameters were as follows: Gas temp. 80 °C, gas flow 15 L/min (N_2), nebulizer 30 psi, sheath gas heater 275 °C, sheath gas flow 11 L/min (N_2), capillary voltage 2500 V and nozzle voltage 500 V. The fragmentor voltage was 380 V. Delta EMV was set to 500. For the analysis, we used a *Poroshell 120 SB-C8* column from *Agilent* (2.7 μm, 2.1 mm × 150 mm). The column temperature was maintained at 30 °C. The flow rate was 0.35 mL min^{-1}, and the injection volume amounted to 39 μL. The effluent up to 1.0 min and after 9 min was diverted to waste by a *Valco* valve in order to protect the mass spectrometer. The auto-sampler was cooled to 4 °C.

The dC- and dG-content of DNA samples was determined by LC-UV-detection. The compounds were separated by a gradient using water (0.0090 % *v/v* formic acid) and MeCN (0.0075 % *v/v* formic acid): 0→5 min; 0→3.5 % (*v/v*) MeCN; 5→6.9 min; 3.5→5% MeCN; 6.9→7.2 min; 5→80 % MeCN; 7.2→10.5 min; 80 % MeCN; 10.5→11.3 min; 80→0% MeCN; 11.3→

13 min; 0% MeCN. In addition to our previously reported UHPLC-MS parameters, we implemented parameters for H_2–AzadC in time segment 1.0–4.0 min with a Quantifier and a Qualifier fragmentation (*Table SI-1*).

For RNA samples, the amount of the canonical RNA nucleosides A, C, G, and U was determined by LC-UV detection. For analysis of the H_2–AzaC content of RNA, the compounds were separated by a gradient using water and MeCN, each containing 0.0090% (*v/v*) formic acid: 0→2 min, 0→0% (*v/v*) MeCN; 2→6 min, 0→6% MeCN; 6→7 min, 6→40% MeCN; 7→10.8 min, 40→80% MeCN; 10.8→20 min, 80% MeCN; 20→20.8 min, 80→0% MeCN; 20.8→22 min, 0% MeCN. We implemented UHPLC-MS parameters for H_2–AzaC in time segment 0.8–2.7 min with a Quantifier and a Qualifier fragmentation (*Table SI-2*).

For absolute quantification of H_2–AzadC and H_2–AzaC, we used calibration curves of diluted standards that were measured in technical triplicate prior to every batch (*Figure SI-10*). Each dilution was subjected to the same digest conditions as the DNA or RNA samples to compensate for strong ion suppression of the MS-signal. The resulting calibration curves were then used for quantitation of the samples from the according batch. For each calibration curve, the lower limit of quantification (LLOQ) was defined as the limit, where backfit of the calibration equation was out of a 80%–120% range (*Table SI-3*), and %CV of the median MS-signal was below 15%.

Stability of DNA-Integrated AzadC

In a stability test, we aliquoted a treated, but not reduced DNA sample into two vials, of which we froze one at −20 °C and incubated the other one for 24 h at r.t. After the incubation time, both samples were treated with $NaBH_4$ as described and the re-isolated DNA was digested in technical triplicates. The levels of H_2-AzadC were determined (*Figure SI-15*).

Statistical Analysis

UHPLC-ESI-MS/MS data were obtained from three independent biological experiments (unless stated otherwise). Each biological data point was measured as technical triplicate. Error bars represent standard deviation of three independent experiments. Statistical analysis (*Tables SI-8–SI-10*) was performed with SigmaPlot® software version 11.0 (*Systat Software Inc.*, Chicago, USA), using One-Way ANOVA *Holm-Sidak* as test. Statistical significance is assumed if as * for $p \leq 0.05$, ** for $p \leq 0.01$ and as *** for $p \leq 0.001$.

Acknowledgements

We thank the *Deutsche Forschungsgemeinschaft*, SFB1032, SFB1309, SPP1784 and the *Excellence Cluster CiPS^M* for financial support. Further support is acknowledged from the *Fonds der Chemischen Industrie* (predoctoral fellowship to *M. S.*).

Author Contribution Statement

S. S. and *T. M. W.* contributed equally to this publication and conducted the experiments. *M. S.* helped with Orbitrap MS and *K. I.* developed the method for quantification of m^5C. *M. M.* and *T. C.* designed the experiments. *S. S.*, *T. M. W.*, *M. M.* and *T. C.* wrote the manuscript.

References

[1] A. Bird, 'DNA methylation patterns and epigenetic memory', *Genes Dev.* **2002**, *16*, 6–21.
[2] A. Gupta, A. K. Godwin, L. Vanderveer, A. Lu, J. Liu, 'Hypomethylation of the synuclein gamma gene CpG island promotes its aberrant expression in breast carcinoma and ovarian carcinoma', *Cancer Res.* **2003**, *63*, 664–673.
[3] B. Thienpont, J. Steinbacher, H. Zhao, F. D'Anna, A. Kuchnio, A. Ploumakis, B. Ghesquière, L. Van Dyck, B. Boeckx, L. Schoonjans, E. Hermans, F. Amant, V. N. Kristensen, K. Peng Koh, M. Mazzone, M. Coleman, T. Carell, P. Carmeliet, D. Lambrechts, 'Tumour hypoxia causes DNA hypermethylation by reducing TET activity', *Nature* **2016**, *537*, 63–68.
[4] N. Gangat, M. M. Patnaik, A. Tefferi, 'Myelodysplastic syndromes: Contemporary review and how we treat', *Am. J. Hematol.* **2016**, *91*, 76–89.
[5] H. Kantarjian, J. P. J. Issa, C. S. Rosenfeld, J. M. Bennett, M. Albitar, J. DiPersio, V. Klimek, J. Slack, C. de Castro, F. Ravandi, R. Helmer III, L. Shen, S. D. Nimer, R. Leavitt, A. Raza, H. Saba, 'Decitabine improves patient outcomes in myelodysplastic syndromes: results of a phase III randomized study', *Cancer* **2006**, *106*, 1794–1803.
[6] P. Fenaux, G. J. Mufti, E. Hellstrom-Lindberg, V. Santini, C. Finelli, A. Giagounidis, R. Schoch, N. Gattermann, G. Sanz, A. List, S. D. Gore, J. F. Seymour, J. M. Bennett, J. Byrd, J. Backstrom, L. Zimmerman, D. McKenzie, C. L. Beach, L. R. Silverman, 'Efficacy of azacitidine compared with that of conventional care regimens in the treatment of higher-risk myelodysplastic syndromes: a randomised, open-label, phase III study', *Lancet Oncol.* **2009**, *10*, 223–232.

[7] L. H. Li, E. J. Olin, H. H. Buskirk, L. M. Reineke, 'Cytotoxicity and mode of action of 5-azacytidine on L1210 leukemia', *Cancer Res.* **1970**, *30*, 2760–2769.
[8] E. Flatau, F. A. Gonzales, L. A. Michalowsky, P. A. Jones, 'DNA methylation in 5-aza-2′-deoxycytidine-resistant variants of C3H 10T1/2 C18 cells', *Mol. Cell. Biol.* **1984**, *4*, 2098–2102.
[9] J. K. Christman, '5-Azacytidine and 5-aza-2′-deoxycytidine as inhibitors of DNA methylation: mechanistic studies and their implications for cancer therapy', *Oncogene* **2002**, *21*, 5483–5495.
[10] R. Jüttermann, E. Li, R. Jaenisch, 'Toxicity of 5-aza-2′-deoxycytidine to mammalian cells is mediated primarily by covalent trapping of DNA methyltransferase rather than DNA demethylation', *Proc. Natl. Acad. Sci. USA* **1994**, *91*, 11797–11801.
[11] D. Kuch, L. Schermelleh, S. Manetto, H. Leonhardt, T. Carell, 'Synthesis of DNA Dumbbell Based Inhibitors for the Human DNA Methyltransferase Dnmt1', *Angew. Chem. Int. Ed.* **2008**, *47*, 1515–1518.
[12] L. Schermelleh, F. Spada, H. P. Easwaran, K. Zolghadr, J. B. Margot, M. C. Cardoso, H. Leonhardt, 'Trapped in action: direct visualization of DNA methyltransferase activity in living cells', *Nat. Methods* **2005**, *2*, 751–756.
[13] P. A. Jones, S. M. Taylor, 'Cellular differentiation, cytidine analogs and DNA methylation', *Cell* **1980**, *20*, 85–93.
[14] M. Daskalakis, T. T. Nguyen, C. Nguyen, P. Guldberg, G. Köhler, P. Wijermans, P. A. Jones, M. Lübbert, 'Demethylation of a hypermethylated P15/INK4B gene in patients with myelodysplastic syndrome by 5-Aza-2′-deoxycytidine (decitabine) treatment', *Blood* **2002**, *100*, 2957–2964.
[15] M. S. Soengas, P. Capodieci, D. Polsky, J. Mora, M. Esteller, X. Opitz-Araya, R. McCombie, J. G. Herman, W. L. Gerald, Y. A. Lazebnik, C. Cordón-Cardó, S. W. Lowe, 'Inactivation of the apoptosis effector *Apaf-1* in malignant melanoma', *Nature* **2001**, *409*, 207–211.
[16] M. G. Goll, F. Kirpekar, K. A. Maggert, J. A. Yoder, C.-L. Hsieh, X. Zhang, K. G. Golic, S. E. Jacobsen, T. H. Bestor, 'Methylation of $tRNA^{Asp}$ by the DNA Methyltransferase Homolog Dnmt2', *Science* **2006**, *311*, 395–398.
[17] S. Hussain, A. A. Sajini, S. Blanco, S. Dietmann, P. Lombard, Y. Sugimoto, M. Paramor, J. G. Gleeson, D. T. Odom, J. Ule, M. Frye, 'NSun2-Mediated Cytosine-5 Methylation of Vault Noncoding RNA Determines Its Processing into Regulatory Small RNAs', *Cell Rep.* **2013**, *4*, 255–261.
[18] Y. Cámara, J. Asin-Cayuela, C. B. Park, M. D. Metodiev, Y. Shi, B. Ruzzenente, C. Kukat, B. Habermann, R. Wibom, K. Hultenby, T. Franz, H. Erdjument-Bromage, P. Tempst, B. M. Hallberg, C. M. Gustafsson, N. G. Larsson, 'MTERF4 Regulates Translation by Targeting the Methyltransferase NSUN4 to the Mammalian Mitochondrial Ribosome', *Cell Metab.* **2011**, *13*, 527–539.
[19] S. Haag, A. S. Warda, J. Kretschmer, M. A. Günnigmann, C. Höbartner, M. T. Bohnsack, 'NSUN6 is a human RNA methyltransferase that catalyzes formation of m^5C72 in specific tRNAs', *RNA* **2015**, *21*, 1532–1543.
[20] R. Itzykson, O. Kosmider, T. Cluzeau, V. Mansat-De Mas, F. Dreyfus, O. Beyne-Rauzy, B. Quesnel, N. Vey, V. Gelsi-Boyer, S. Raynaud, C. Preudhomme, L. Adès, P. Fenaux, M. Fontenay, 'Impact of *TET2* mutations on response rate to azacitidine in myelodysplastic syndromes and low blast count acute myeloid leukemias', *Leukemia* **2011**, *25*, 1147–1152.
[21] R. Itzykson, O. Kosmider, A. Renneville, V. Gelsi-Boyer, M. Meggendorfer, M. Morabito, C. Berthon, L. Adès, P. Fenaux, O. Beyne-Rauzy, N. Vey, T. Braun, T. Haferlach, F. Dreyfus, N. C. P. Cross, C. Preudhomme, O. A. Bernard, M. Fontenay, W. Vainchenker, S. Schnittger, D. Birnbaum, N. Droin, E. Solary, 'Prognostic Score Including Gene Mutations in Chronic Myelomonocytic Leukemia', *J. Clin. Oncol.* **2013**, *31*, 2428–2436.
[22] R. Bejar, A. Lord, K. Stevenson, M. Bar-Natan, A. Pérez-Ladaga, J. Zaneveld, H. Wang, B. Caughey, P. Stojanov, G. Getz, G. Garcia-Manero, H. Kantarjian, R. Chen, R. M. Stone, D. Neuberg, D. P. Steensma, B. L. Ebert, '*TET2* mutations predict response to hypomethylating agents in myelodysplastic syndrome patients', *Blood* **2014**, *124*, 2705–2712.
[23] M. Xie, Q. Jiang, Y. Xie, 'Comparison Between Decitabine and Azacitidine for the Treatment of Myelodysplastic Syndrome: A Meta-Analysis With 1392 Participants', *Clin. Lymphoma Myeloma Leuk.* **2015**, *15*, 22–28.
[24] K.-T. Lin, R. L. Momparlerm, G. E. Rivard, 'High-performance Liquid Chromatographic Analysis of Chemical Stability of 5-aza-2′-Deoxycytidine', *J. Pharm. Sci.* **1981**, *70*, 1228–1232.
[25] D. K. Rogstad, J. L. Herring, J. A. Theruvathu, A. Burdzy, C. C. Perry, J. W. Neidigh, L. C. Sowers, 'Chemical Decomposition of 5-aza-2′-deoxycytidine (Decitabine): Kinetic Analyses and Identification of Products by NMR, HPLC, and Mass Spectrometry', *Chem. Res. Toxicol.* **2009**, *22*, 1194–1204.
[26] S. Öz, G. Raddatz, M. Rius, N. Blagitko-Dorfs, M. Lübbert, C. Maercker, F. Lyko, 'Quantitative determination of decitabine incorporation into DNA and its effect on mutation rates in human cancer cells', *Nucleic Acids Res.* **2014**, *42*, e152.
[27] T. Qin, J. Jelinek, J. Si, J. Shu, J.-P. Issa, 'Mechanisms of resistance to 5-aza-2′-deoxycytidine in human cancer cell lines', *Blood* **2009**, *113*, 659–667.
[28] N. M. Anders, J. Liu, T. Wanjiku, H. Giovinazzo, J. Zhou, A. Vaghasia, W. G. Nelson, S. Yegnasubramanian, M. A. Rudek, 'Simultaneous quantitative determination of 5-aza-2′-deoxycytidine genomic incorporation and DNA demethylation by liquid chromatography tandem mass spectrometry as exposure-response measures of nucleoside analog DNA methyltransferase inhibitors', *J. Chromatogr. B* **2016**, *1022*, 38–45.
[29] M. Matoušová, I. Votruba, M. Otmar, E. Tloušťová, J. Günterová, H. Mertlíková-Kaiserová, '2′-deoxy-5,6-dihydro-5-azacytidine – a less toxic alternative of 2′-deoxy-5-azacytidine: a comparative study of hypomethylating potential', *Epigenetics* **2011**, *6*, 769–776.
[30] J. A. Beisler, M. M. Abbasi, J. A. Kelley, J. S. Driscoll, 'Synthesis and antitumor activity of dihydro-5-azacytidine, a hydrolytically stable analogue of 5-azacytidine', *J. Med. Chem.* **1977**, *20*, 806–812.
[31] A. Unnikrishnan, A. N. Q. Vo, R. Pickford, M. J. Raftery, A. C. Nunez, A. Verma, L. B. Hesson, J. E. Pimanda, 'AZA-MS: a novel multiparameter mass spectrometry method to determine the intracellular dynamics of azacitidine therapy *In Vivo*', *Leukemia* **2018**, *32*, 900–910.

[32] K. S. Harris, W. Brabant, S. Styrchak, A. Gall, R. Daifuku, 'KP-1212/1461, a nucleoside designed for the treatment of HIV by viral mutagenesis', *Antiviral Res.* **2005**, *67*, 1–9.

[33] T. Pfaffeneder, F. Spada, M. Wagner, C. Brandmayr, S. K. Laube, D. Eisen, M. Truss, J. Steinbacher, B. Hackner, O. Kotljarova, D. Schuermann, S. Michalakis, O. Kosmatchev, S. Schiesser, B. Steigenberger, N. Raddaoui, G. Kashiwazaki, U. Müller, C. G. Spruijt, M. Vermeulen, H. Leonhardt, P. Schär, M. Müller, T. Carell, 'Tet oxidizes thymine to 5-hydroxymethyluracil in mouse embryonic stem cell DNA', *Nat. Chem. Biol.* **2014**, *10*, 574–581.

[34] G. Ficz, T. A. Hore, F. Santos, H. J. Lee, W. Dean, J. Arand, F. Krueger, D. Oxley, Y.-L. Paul, J. Walter, S. J. Cook, S. Andrews, M. R. Branco, W. Reik, 'FGF Signaling Inhibition in ESCs Drives Rapid Genome-wide Demethylation to the Epigenetic Ground State of Pluripotency', *Cell Stem Cell* **2013**, *13*, 351–359.

[35] E. Habibi, A. B. Brinkman, J. Arand, L. I. Kroeze, H. H. Kerstens, F. Matarese, K. Lepikhov, M. Gut, I. Brun-Heath, N. C. Hubner, R. Benedetti, L. Altucci, J. H. Jansen, J. Walter, I. G. Gut, H. Marks, H. G. Stunnenberg, 'Whole-Genome Bisulfite Sequencing of Two Distinct Interconvertible DNA Methylomes of Mouse Embryonic Stem Cells', *Cell Stem Cell* **2013**, *13*, 360–369.

[36] H. G. Leitch, K. R. McEwen, A. Turp, V. Encheva, T. Carroll, N. Grabole, W. Mansfield, B. Nashun, J. G. Knezovich, A. Smith, M. A. Surani, P. Hajkova, 'Naive pluripotency is associated with global DNA hypomethylation', *Nat. Struct. Mol. Biol.* **2013**, *20*, 311–316.

[37] J. Aimiuwu, H. Wang, P. Chen, Z. Xie, J. Wang, S. Liu, R. Klisovic, A. Mims, W. Blum, G. Marcucci, K. K. Chan, 'RNA-dependent inhibition of ribonucleotide reductase is a major pathway for 5-azacytidine activity in acute myeloid leukemia', *Blood* **2012**, *119*, 5229–5238.

[38] D. Biniszkiewicz, J. Gribnau, B. Ramsahoye, F. Gaudet, K. Eggan, D. Humpherys, M.-A. Mastrangelo, Z. Jun, J. Walter, R. Jaenisch, '*Dnmt1* Overexpression Causes Genomic Hypermethylation, Loss of Imprinting, and Embryonic Lethality', *Mol. Cell. Biol.* **2002**, *22*, 2124–2135.

[39] S. J. Collins, R. C. Gallo, R. E. Gallagher, 'Continuous growth and differentiation of human myeloid leukaemic cells in suspension culture', *Nature* **1977**, *270*, 347–349.

[40] R. Gallagher, S. Collins, J. Trujillo, K. McCredie, M. Ahearn, S. Tsai, R. Metzgar, G. Aulakh, R. Ting, F. Ruscetti, R. Gallo, 'Characterization of the continuous, differentiating myeloid cell line (HL-60) from a patient with acute promyelocytic leukemia', *Blood* **1979**, *54*, 713–733.

[41] Y. Matsuo, R. A. F. MacLeod, C. C. Uphoff, H. G. Drexler, C. Nishizaki, Y. Katayama, G. Kimura, N. Fujii, E. Omoto, M. Harada, K. Orita, 'Two acute monocytic leukemia (AML–M5a) cell lines (MOLM-13 and MOLM-14) with interclonal phenotypic heterogeneity showing MLL-AF9 fusion resulting from an occult chromosome insertion, ins (11;9)(q23;p22p23)', *Leukemia* **1997**, *11*, 1469–1477.

[42] E. Li, T. H. Bestor, R. Jaenisch, 'Targeted mutation of the DNA methyltransferase gene results in embryonic lethality', *Cell* **1992**, *69*, 915–926.

[43] H. Lei, S. P. Oh, M. Okano, R. Jüttermann, K. A. Goss, R. Jaenisch, E. Li, 'De novo DNA cytosine methyltransferase activities in mouse embryonic stem cells', *Development* **1996**, *122*, 3195–3205.

[44] M. Okano, S. Xie, E. Li, 'Dnmt2 is not required for *de novo* and maintenance methylation of viral DNA in embryonic stem cells', *Nucleic Acids Res.* **1998**, *26*, 2536–2540.

[45] M. J. Booth, G. Marsico, M. Bachman, D. Beraldi, S. Balasubramanian, 'Quantitative sequencing of 5-formylcytosine in DNA at single-base resolution', *Nat. Chem.* **2014**, *6*, 435–440.

[46] D. Globisch, M. Münzel, M. Müller, S. Michalakis, M. Wagner, S. Koch, T. Brückl, M. Biel, T. Carell, 'Tissue Distribution of 5-Hydroxymethylcytosine and Search for Active Demethylation Intermediates', *PLoS One* **2010**, *5*, e15367.

[47] M. Münzel, D. Globisch, T. Brückl, M. Wagner, V. Welzmiller, S. Michalakis, M. Müller, M. Biel, T. Carell, 'Quantification of the Sixth DNA Base Hydroxymethylcytosine in the Brain', *Angew. Chem. Int. Ed.* **2010**, *49*, 5375–5377.

[48] S. Schiesser, T. Pfaffeneder, K. Sadeghian, B. Hackner, B. Steigenberger, A. S. Schröder, J. Steinbacher, G. Kashiwazaki, G. Höfner, K. T. Wanner, C. Ochsenfeld, T. Carell, 'Deamination, Oxidation, and C–C Bond Cleavage Reactivity of 5-Hydroxymethylcytosine, 5-Formylcytosine, and 5-Carboxycytosine', *J. Am. Chem. Soc.* **2013**, *135*, 14593–14599.

Received December 7, 2018
Accepted January 10, 2019

